



AKADÉMIAI KIADÓ

Pollack Periodica •  
An International Journal  
for Engineering and  
Information Sciences

18 (2023) 2, 48–53

DOI:  
[10.1556/606.2022.00680](https://doi.org/10.1556/606.2022.00680)  
© 2022 The Author(s)

ORIGINAL RESEARCH  
PAPER



\*Corresponding author.  
E-mail: [muhanad.kh.99.oo@gmail.com](mailto:muhanad.kh.99.oo@gmail.com)



AKJournals

# The effectiveness parameters analysis for piers scour calculation

Muhanad AL-Jubouri\*  and Richard P. Ray

Department of Structural and Geotechnical Engineering, Faculty of Architecture, Civil, and Transportation Engineering, Széchenyi István University, Győr, Hungary

Received: June 14, 2022 • Revised manuscript received: November 5, 2022 • Accepted: December 11, 2022  
Published online: March 22, 2023

## ABSTRACT

A computational fluid dynamics numerical model addressed the problem of local scouring and deposition calculation for non-cohesive sediment and clear water conditions near single and double cylindrical piers. The numerical results of single cylindrical piers correlate very well with the physical model's results while are higher than the case of the double pier, especially when the large-eddy turbulence model, the van Rijn bed-load transport equation, and fine mesh size are considered. Additionally, the final numerical predictions are compared to experimental data after parameters effectiveness explores the range of results based on projected user inputs like the bed-load equation, mesh cell size, and turbulence model.

## KEYWORDS

local scouring, non-cohesive, clear water, computational fluid dynamics, turbulence model, bed-load equation

## 1. INTRODUCTION

A local scour is the most crucial among the different forms of scours that affect bridge operation and safety. Bridge scour is produced by rushing water's erosive action, excavating, and transporting sediments from the piers' surroundings. It is caused by constructions interfering with river flows and is defined by the emergence of a scour hole around bridge piers. Consequently, even though much time, cost, and energy have gone into anticipating bridge scour so that early hazard warnings may be given, studying scour development at piers is still challenging, especially in three-dimensional space. Flows beneath hydraulic structures in the standard mobile-bed streams have varying geometric complexity due to the intrinsic morphologic abundance of bed bathymetry and a diverse range of hydraulic structures like bridge piers. Energetic, consistent vertical structures control them. Vortices interface with sediments on the stream bed, causing local scour, which might compromise streambed stabilization and the structural dependability of embedded hydraulic systems [1].

For bridge pier stability investigation, the progressive development of the scouring procedure and the characterization of the loads applied on bridge piers are crucial. It should be comprehensively investigated, like under-estimation of scour depth can result in structural collapse, while over-prediction can waste financial resources. As a result, detailed knowledge of the scour procedure and a more accurate calculation of the scour cavity geometry dimensions are critical in civil engineering. The physical study, numerical simulations, and analytical solutions have all been presented as methods and methodologies for studying local scour near bridge piers [2–5]. Nevertheless, many approaches have flaws that limit their accuracy in real-world applications. Experimental scour testing, for example, can only be carried out for a few major bridge projects due to their high cost and labor intensity.

Analytical solutions are suggested in current design guidelines because of their practical conveniences and economic benefits [6]. The most considerable challenge for these analytical methods is ensuring the veracity of the assumptions and simplifications adopted for intricate

bridge instances. Almost all analytical solutions, for example, are based on the assumption that scours events are limited to a one-dimensional condition with only one parameter, namely the scour depth. Because of the horseshoe vortex structure's strong three-Dimensional (3D) character, these conventional approaches for measuring scour may be insufficient to forecast the physical processes generating scour holes at bridges [7].

Computational Fluid Dynamics (CFD) is a prevailing apparatus for simulating complex hydraulic scenarios, as those found around existing bridge infrastructure, and it offers a viable option for minimizing some of the uncertainty associated with traditional scour research approaches. Most researchers have revealed that this dimensions mismatch can cause a big mistake in the scour computation [8–10]. As a result, the 3D scour simulation technique is recently grown popular. However, two concerns must be addressed before these 3D simulations can be used in practice. First, according to reference [11], the flow field boundary used in bridge scour simulations was typically predetermined patterns (some existing functions) and the virtual immersed boundary, which hardly matches the actual conditions. Secondly, commercial CFD tools should be redeveloped to give a particular simulation aimed at bridge scour [12]. Numerical simulation can model complex problems that are difficult to model under laboratory circumstances.

This research aims to contribute to the numerical analysis of the flow and scouring processes near bridge piers to prove that the sediment transport model can accurately forecast scouring and deposition trends at bridge piers and put a variety of user-defined input factors to the test to see how effective the final scour as deposition trends are to them. In this project numerical techniques are utilized to solve fluid flow equations for transient and three-dimensional resolutions to obtain multi-scale multi-physics flow issues. As a result, users can use this model for a broad range of fluid flows and thermal performance phenomena thanks to the combination of physical and numerical options, and it is frequently used to solve various hydraulic difficulties. The validation of numerical simulation by laboratory models of [13] is used to compare the findings of a physical prototype of local scour around the single and double cylindrical piers with a numerical model of the CFD program for verification.

## 2. EXPERIMENTAL MODEL

The numerical model was authenticated using experimental archives from the physical model given in [13] at the Coimbra University. Utilizing an Acoustic Doppler Velocimeter (ADV) and a Moulinet, the velocity, and flow rate of the water flow were determined and estimated. Cylindrical-shaped piers were used to estimate optimum scour depth and deposition trends. The experimental flume is 7.5 m long, 0.3 m wide, and 0.5 m deep. A 5 cm depth and 190 cm long of uniformly graded non-cohesive sand with a  $D_{50} = 0.27$  mm were provided in the flume. When the sand was prepared,

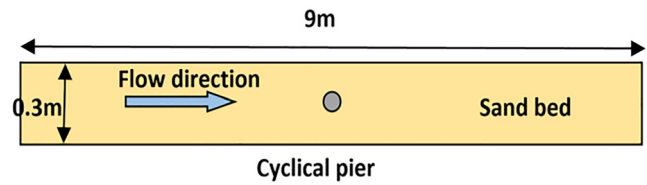


Fig. 1. The flume schematic (Source: modified from [13])

the flume was pumped with water to the initial depth equal to 8 cm. The experimental set-up featured an average inflow velocity of  $0.0868 \text{ m s}^{-1}$  and a uniform flow depth of 10.5 cm for a 4 cm diameter of the cylindrical pier. The flume schematic is shown in Fig. 1.

## 3. NUMERICAL MODEL AND TURBULENCE MODEL

Many natural systems are modeled using computer simulations in various research and engineering sectors. In addition, simulations can estimate system performance when analytical solutions are too complex [14].

### 3.1. The continuity equation, the momentum conservation, and the Navier-Stokes equations

The continuity equation and the momentum conservation equations are the equations that control the motion of a viscous fluid. The Navier-Stokes equations are the name for these equations. For uncompressed viscous liquids, the Navier-Stokes and continuity can be written as follows:

$$\frac{\partial \bar{u}_i}{\partial \bar{x}_i} = 0, \quad (1)$$

$$\frac{\partial \bar{u}_i}{\partial t} + \frac{\partial \bar{u}_i \bar{u}_j}{\partial \bar{x}_j} = \frac{1}{\rho} \frac{\partial \bar{P}}{\partial \bar{x}_i} + \vartheta \left( \frac{\partial^2 \bar{u}_i}{\partial \bar{x}_j^2} \right) + \left( \frac{\partial \tau_{ij}}{\partial \bar{x}_j} \right), \quad (2)$$

where  $x_i$  designates the stream-wise, timeframe, and vertical directions;  $\bar{P}$  is the time-averaged or filtered pressure;  $\bar{u}_i, \bar{u}_j$  are the time-averaged in both the directions;  $\rho$  is the fluid's density;  $\tau_{ij}$  is the Reynolds shear stress and  $\vartheta$  is the kinematic viscosity [14].

### 3.2. Renormalized group standard

The ReNormalized Group (RNG) is reorganized to produce a two-equation ( $k$ ) model. The  $k$  model, which is critical for predicting the consequences of turbulence, is the foundation concept for observing Reynold's stress and viscous stress. The RNG ( $k$ -model) is a more robust variant of the two-equation  $k$ - $\epsilon$  model and is recommended for most industrial issues. It improves the coverage of transitionally-turbulent flows, curved flows, wall heat transfer, and mass transfer by extending the capabilities of the primary  $k$ -model [15],

$$v_i = C_\mu \frac{k^2}{\epsilon}. \quad (3)$$



The standard  $k$ - $\varepsilon$  can be determined through these two equations:

$$\begin{aligned} \frac{\partial k}{\partial t} + u_i \frac{\partial k}{\partial x_i} &= \frac{\partial}{\partial x_i} \left( \frac{\nu}{\sigma_k} \frac{\partial k}{\partial x_i} \right) + v_i \left( \frac{\partial u_i}{\partial x_j} + \frac{\partial u_j}{\partial x_i} \right) \frac{\partial u_i}{\partial x_j} - \varepsilon, \quad (4) \\ \frac{\partial \varepsilon}{\partial t} + u_i \frac{\partial \varepsilon}{\partial x_i} &= \frac{\partial}{\partial x_i} \left( \frac{\nu_t}{\sigma_\varepsilon} \frac{\partial \varepsilon}{\partial x_i} \right) + C_1 \frac{\varepsilon}{k} v_t \left( \frac{\partial u_i}{\partial x_j} + \frac{\partial u_j}{\partial x_i} \right) \frac{\partial u_i}{\partial x_j} \\ &\quad - C_2 \frac{\varepsilon^2}{k}, \quad (5) \end{aligned}$$

where  $C_\mu$  is an empirical coefficient;  $k$  and  $\varepsilon$  are the kinetic energy and dissipation, respectively.  $C_1 = 1.44$ ,  $C_2 = 1.92$ ,  $\sigma_k = 1.3$  and  $\sigma_\varepsilon = 1.3$ .

### 3.3. The large eddy simulation model

In computation fluid dynamics, one turbulence model choice is the Large Eddy Simulation (LES) model. This equipment can reduce computing costs by ignoring the minor length scales, which are the most expensive to resolve in most computations. The LES model resolves most turbulent fluctuations directly rather than scalars to describe turbulent kinetic energy. It necessitates a significantly more satisfactory mesh resolution than two-equation models and gives more detailed information on turbulent flow. The LES is more computationally intensive than the RNG models by employing advanced computer technology. Its application will become more widespread. According to reference [16], the LES turbulence employing the van Rijn sediment transport models proves more effective with mesh matrices and is adequate compared to other options. The LES kinematic eddy viscosity ( $\nu_T$ ) behaves as [16]:

$$\nu_T = (cL)^2 \sqrt{2e_{ij}2e_{ji}}, \quad (6)$$

where  $c$  is a constant value between 0.1–0.2;  $e_{ij}$  is the strain rate tensor components in the  $i$  and  $j$  directions, and  $L$  is the length scale.

## 4. THE BED-LOAD EQUATIONS

One of the most significant factors for calculating scour is the sediment transfer rate; precise scouring forecasts may be accomplished by changing the sediment transport equations. There are three options to compute the dimensionless bed load transfer as follows:

i) Mayer-Peter and Muller [17]:

$$\Phi_i = \beta_M \left( \theta_i - \theta'_{cb,i} \right)^{1.5} C_b; \quad (7)$$

ii) van Rijn [18]

Because non-cohesive sediment was employed in this investigation, the van Rijn equation was used to obtain the dimensionless bed load transfer rate:

$$\Phi_i = \beta_V d_*^{-0.3} \left( \frac{\theta}{\theta_{cr}} - 1 \right)^{2.1} C_b; \quad (8)$$

iii) Nilsen [19]:

$$\Phi_i = \beta_N \theta_i^{0.5} \left( \theta_i - \theta'_{cb,i} \right) C_b, \quad (9)$$

where  $\Phi_i$  is the dimensionless bed-load transport rate proportional to the volumetric bed-load transport rate used to compute the bed-load transport in units of volume per bed width per time  $q_b$ . ( $\beta_M$ ,  $\beta_V$  and  $\beta_N$ .) are the coefficients typically 8.0, 0.053, and 12.0, respectively.

## 5. THE LOCAL SCOUR SIMULATIONS PROCESSES

Pier configurations were set up in the numerical model to reflect the physical model's circumstances. The sediment transport simulations began with completing steady-state solutions for the hydraulics only, which served as the simulation's beginning condition. A single sediment species with a diameter of 0.27 mm and a density is  $2,650 \text{ kg m}^{-3}$  was used to activate the sediment model. The computational mesh was designed with a uniform cell size of 0.005 m, and the domain with full ranges allowed for more satisfactory resolution in the study region. Several essential parameters that directly impact the results were calibrated after validating the percentage of conformity of numerical results with laboratory results. The calibrated values of parameters were employed in the numerical simulation. In this investigation, boundary conditions were applied. The specific velocity ( $V$ ) boundary was placed at the intake, the water velocity was  $0.0868 \text{ m s}^{-1}$ , and the water depth was 0.101 m. The boundary was identified as outflow ( $O$ ) at the downstream, bottom, and lateral walls corresponding to sidewalls; no-slip boundary requirements were given, resulting in zero tangential velocity at the solid surfaces. Stagnation pressure and zero fraction fluid were applied to the free surface,  $Z_{\max}$ . The numerical model's boundary conditions should match the physical circumstances of the problem. The critical model set-up inputs are the large-eddy turbulence model, the van Rijn bed-load transfer equation, second-order momentum advection, the surface roughness,  $d_{50}$  equal to 1, and a critical shield number is 0.024.

Through the Fractional Area/Volume Obstacle Representation (FAVOR) the CFD program has a very simple, quicker, but strong meshing capability of FAVOR. This technique accurately describes complicated characteristics in the computational domain without needing a fitted grid. It employs various techniques to develop numerical stability and calculate interfacial areas, advection, stress, and solid barriers [11]. Simulations were performed until an equilibrium scour depth was reached, and the results were then compared to physical model observations. The approximate run duration for 1800 s of simulation time was 36 h. Identifying empirical connections to quantify the sediment transport mechanisms – bed-load, entrainment, and settling - is a fundamental difficulty in 3D sediment modeling. The selection of proper transport coefficients can be challenging and injects significant uncertainty into the research. The common



variations in bed elevations will result from a complicated series of interactions between the hydraulic solution and the transport processes, which will occur concurrently at each simulation time step. Effectiveness parameters investigation may assess the range of effects for how potential inputs affect the answer. The effectiveness parameters were assumed to examine how cell size, the bed-load transfer equation and critical shield number affect simulation results.

## 6. RESULTS

Figures 2 and 3 illustrate the scour depth and deposition height results and pattern around the single-cylinder pier in three axial directions ( $x,y$ ), ( $y,z$ ), and ( $x,z$ ). The deposition's basic form and pattern are unlike those discovered in the physical model. Due to its geometry irregularity, the researcher runs into an issue when developing the new bridge pier mesh, which meets the requirements for a suitable mesh. To compare the researcher run, the computational modeling under the same hydraulic settings (the Reynolds and stream arrangement) and numerical circumstances (the same eddy viscosity, initial conditions, and identical mesh). The

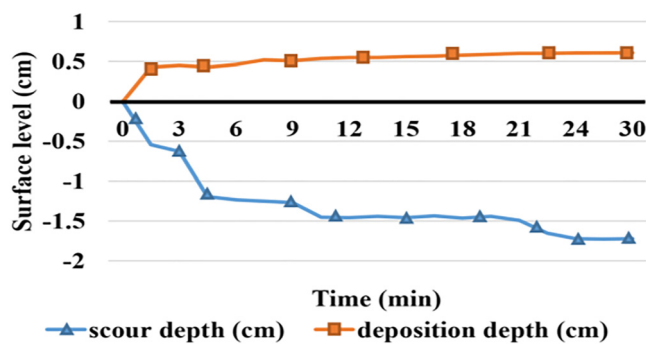


Fig. 2. The scour depth and deposition height around a single cylindrical pier

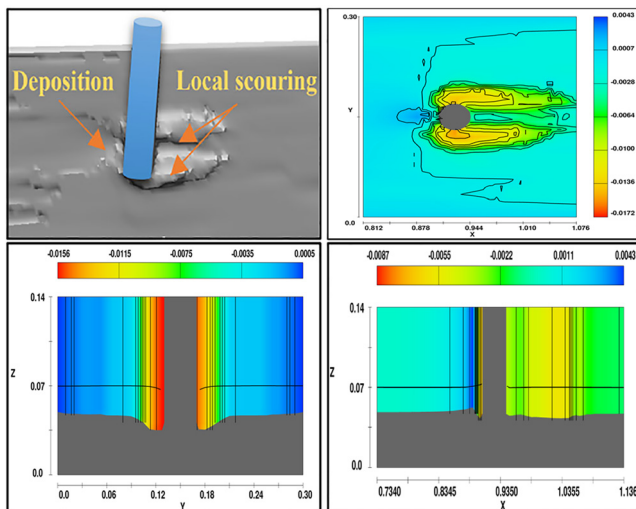


Fig. 3. The scour and deposition pattern of a round single cylindrical pier

modeling approach is the large-eddy with the same model parameters; the computations were run for 30 min until the equilibrium state was reached. The numerical model's conclusions are pretty close to the physical models. The most extraordinary scour depth predicted is 1.73 cm (3.8%) of the recorded value in the experimental test (1.8 cm).

Compared to the observed data, it can be comprehended that the deposition site in the numerical model is pushed downstream. When observed data is compared to estimated data, the scour at the pier's nose is under predicted. Moreover, the expected maximum deposition height of 0.67 cm is within 25% of the observed value of 0.9 cm, indicating general solid agreement with the deposition pattern upstream of the pier.

It is in line with earlier 3D computational models of scour at abrasive piers, and it has been suggested that this is due to vorticity models' failure to resolve the complicated HorseShoe Vortex System (HSVS) adequately [11].

Figures 4 and 5 illustrate the scour depth and deposition height results and pattern around the double-cylindrical pier in three axial directions ( $x,y$ ), ( $y,z$ ), and ( $x,z$ ). The deposition's basic form and pattern are more or less similar to those discovered in the physical model. The numerical model's conclusions agree more with the physical model

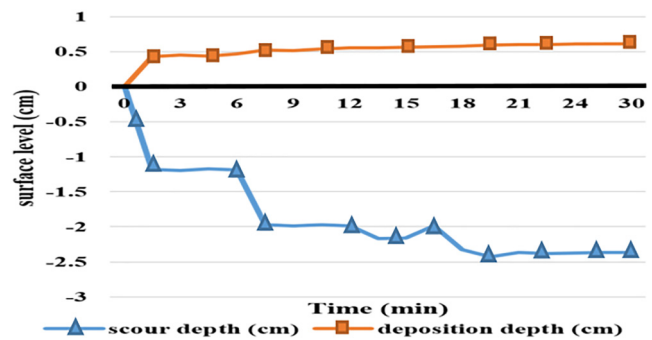


Fig. 4. The scour and deposition depth around the double cylindrical pier

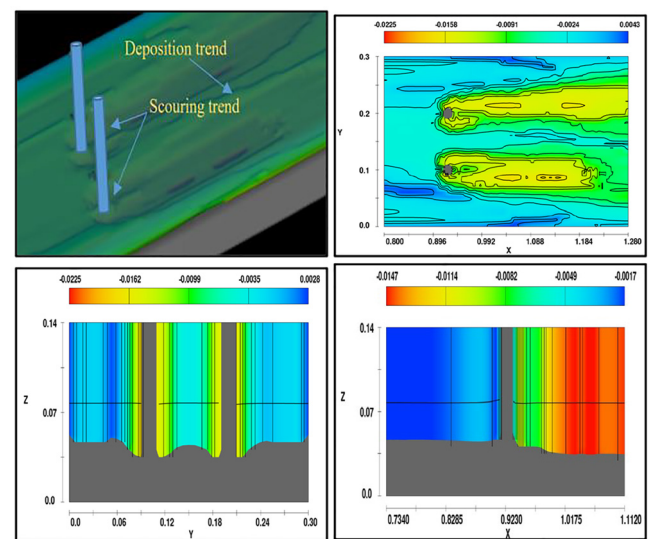


Fig. 5. The scour and deposition pattern of a round double cylindrical pier



than the single pier case regarding scour depth, deposition height, and pattern. The highest scour depth expected is 2.25 cm (20%) of the recorded value in the experimental model of 2.8 cm. Moreover, the estimated maximum deposition height of 0.67 cm is within 68% of the observed value of 2.1 cm, indicating less agreement with the deposition depth and pattern upstream and downstream of the pier. However, the maximum deposition is somewhat downstream compared to the actual data.

## 7. PARAMETERS EFFECTIVENESS ANALYSIS

The impacts of bed-load equation, mesh cell size and turbulence model option on predicted scour depth and height of soil deposition for the single cylindrical pier were inspected using Parameters effectiveness analysis.

Figure 6 shows the results of the bed-load equation effectiveness. The Nielsen, Meyer-Peter Müller, and the van Rijn bed-load equations were used in the simulations, and the results were compared to the experimental findings. These findings demonstrate that the Nielsen and Mayer bed-load equations produced maximum scour forecasts of 25% and 27%, respectively, higher than the van Rijn forecasts. Meyer-Peter and Müller predict that scouring depth is in excellent agreement Nielsen equation. However, the Nielsen, Meyer-Peter and Müller equations yield significantly different trends and shapes for scouring and deposition. The bed-load effectiveness analysis is intriguing since the van

Rijn equation, often employed with the LES turbulence for providing a more precise result, mainly when mesh grids are provided, and is sufficient when compared to other models [16], which produced the best fit with measured data in the current test condition.

In the instance of the circular pier, grid individuality was achieved. The square structured mesh stretches from the sediment bed to the structure. Cells have been defined to discretize the mathematical model. The grid resolution was better altered from coarse to fine to understand a structured grid's influence on numerical results. The simulation model deals with a structured rectangular mesh, which is why it is included in our overall framework. The mesh is one of the influencing aspects in the simulation process, and depending on the number of cells, it might change the operation time. The best computation time values were found using several forms of mesh accuracy. Consequently, different cell sizes of 8, 6, and 5 mm were chosen to determine the best cell size after many trials to satisfy the phenomenon conditions (Fig. 7). Therefore the number of runs performed, as shown in Table 1, to regulate the best cell size selection.

Figure 8 shows the effectiveness analysis results when changing the turbulence model option like the RNG and LES turbulence models. The main findings of the LES simulation model scour formation was observed to be much more fulfilled to the earlier experimental results than the RNG turbulence model also near (Fig. 8). In terms of flow phenomena, the LES simulation model is more realistic. Although the LES simulation can properly replicate the sediment scour in front

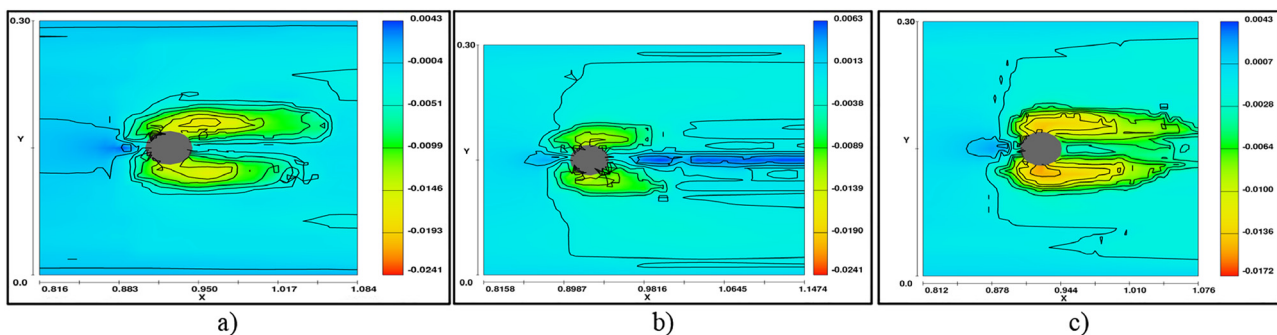


Fig. 6. Scour depth and deposition height anticipated for various bed-load transport equations, a) Nielsen; b) Meyer-Peter and Mueller; c) van Rijn

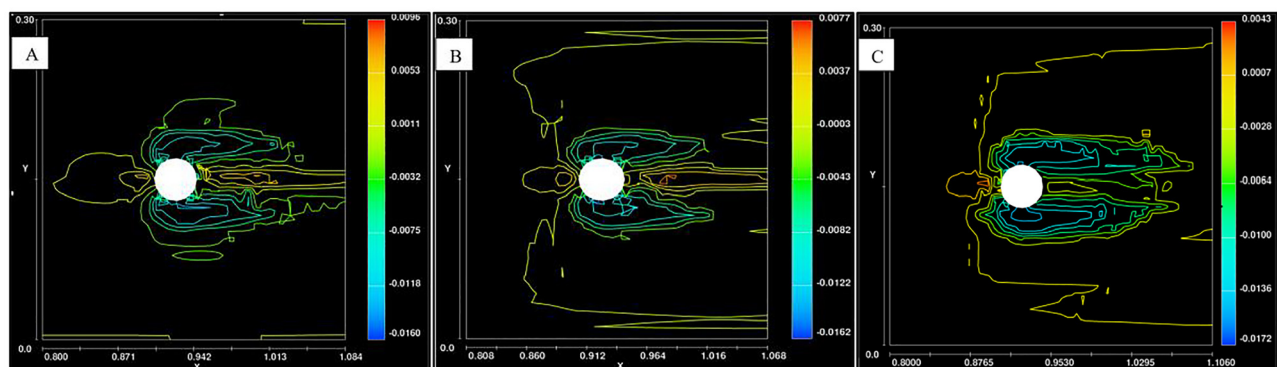


Fig. 7. Scour depth and deposition height is anticipated for various mesh sizes, a) 8 mm; b) 7 mm; and c) 6 mm

Table 1. The size, grid and total number of cells

Cells size (mm)	Grid (X·Y·Z)	Total number of mesh cells
5	1,115·40·29	1,293,400
6	958·40·24	919,680
8	719·40·18	517,680

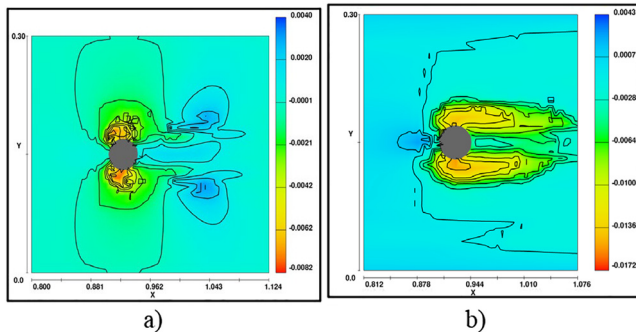


Fig. 8. Scour depth and deposition height are anticipated for a) the RNG and b) the LES turbulence models

of the pier, its implementation will become more prevalent as computer science progresses. The RNG turbulence model resulted in a 50% reduction in scour magnitude forecast. Setting the LES simulation model resulted in a slight rise in the estimated maximum scour depth, but the geographical area of the scour region has expanded dramatically.

## 8. CONCLUSION

The purpose of this study was to confirm the accuracy of this 3D numerical simulation in forecasting the development of the scour depth and deposition height beneath the bridge pier. After 30 min of scour depth running simulation, the verification is completed by comparing the numerical findings with the do Carmo experimental model. The comparison of the results shows that the rate of error for the maximum depth of the scour is equal to 3.8% for single pier case when the large-eddy turbulence model, the van Rijn bed-load transport equation, and fine mesh size are considered while more than this percentage for double pier case. This observation shows a satisfactory validation between the numerical and experimental work, indicating that the numerical simulation correctly reproduces the scour depth.

## REFERENCES

- [1] S. Das, R. Das, and A. Mazumdar, "Circulation characteristics of horseshoe vortex in scour region around circular piers," *Water Sci. Eng.*, vol. 6, no. 1, pp. 59–77, 2013.
- [2] M. Pavúček, J. Rumann, and P. Dušička, "Investigation of scours on a physical model of the Hričov weir using photogrammetry," *Pollack Period.*, vol. 17, no. 1, pp. 105–110, 2022.
- [3] M. Pavúček, J. Rumann, and P. Dušička, "Experimental assessment of secondary stilling basin at the Hričov weir," *Pollack Period.*, vol. 16, no. 2, pp. 67–72, 2021.
- [4] N. B. Singh, T. T. Devi, and B. Kumar, "The local scour around bridge piers - a review of remedial techniques," *ISH J. Hydraulic Eng.*, vol. 28, no. Supl. 1, pp. 527–540, 2020.
- [5] P. Khwairakpam, S. S. Ray, S. Das, R. Das, and A. Mazumdar, "Scour hole characteristics around a vertical pier under clear water scour conditions," *ARNP J. Eng. Appl. Sci.*, vol. 7, no. 6, pp. 649–654, 2012.
- [6] E. V. Richardson, L. J. Harrison, J. R. Richardson, and S. R. Davis, *Evaluating Scour at Bridges*, Hydraulic Engineering Circular, Report no. HEC 18. Federal Highway Administration, 2012.
- [7] M. A. Shahriyar, "Numerical Investigation of Local Scour around Different Shaped Bridge Piers Using Flow 3d Software," Doctoral Thesis. Islamic University of Technology Gazipur, Bangladesh, 2021.
- [8] A. Ghaderi and S. Abbasi, "CFD simulation of local scouring around airfoil-shaped bridge piers with and without collar," *Sādhanā*, vol. 44, no. 10, 2019. Paper no. 216.
- [9] B. W. Melville and S. E. Coleman, *Bridge Scour*. Water Resources Publication, 2000.
- [10] S. Pagliara and I. Carnacina, "Influence of wood debris accumulation on bridge pier scour," *J. Hydraulic Eng.*, vol. 137, no. 2, pp. 254–261, 2011.
- [11] A. Khosronejad, C. Hill, S. Kang, and F. Sotiropoulos, "Computational and experimental investigation of scour past laboratory models of stream restoration rock structures," *Adv. Water Resour.*, vol. 54, pp. 191–207, 2013.
- [12] S. A. H. Sajjadi, S. H. Sajjadi, and H. Sarkardeh, "Accuracy of numerical simulation in asymmetric compound channels," *Int. J. Civ Eng.*, vol. 16, pp. 155–167, 2018.
- [13] J. A. do Carmo, "Experimental study on local scour around bridge piers in rivers," *WIT Trans. Ecol. Environ.*, vol. 83, pp. 3–13, 2005.
- [14] B. C. Chanyal, "Quaternionic approach on the Dirac–Maxwell, Bernoulli and Navier–Stokes equations for dyonic fluid plasma," *Int. J. Mod. Phys. A*, vol. 34, no. 31, 2019, Paper no. 1950202.
- [15] L. Ts. Adzhemyan, T. L. Kim, M. V. Kompaniets, and V. K. Sazonov, "Renormalization group in the infinite-dimensional turbulence: determination of the RG-functions without renormalization constants," *Nanosystems: Phys. Chem. Maths.*, vol. 6, no. 4, pp. 461–469, 2015.
- [16] G. R. Tabor and M. H. Baba-Ahmadi, "Inlet conditions for large eddy simulation: a review," *Comput. Fluids*, vol. 39, no. 4, pp. 553–567, 2010.
- [17] E. Meyer-Peter and R. Muller, "Formulas for bed-load transport," in *Int. Assoc. Hydraul. Struct. Res., 2nd meeting*, Stockholm, Appendix 2, 1948.
- [18] L. C. van Rijn, "Sediment transport, Part I: Bed load transport," *J. Hydraulic Eng.*, vol. 110, no. 10, pp. 1431–1456, 1984.
- [19] P. Nielsen, *Coastal Bottom Boundary Layers and Sediment Transport*. World Scientific, 1992.